

# Large well-relaxed models of vitreous silica, coordination numbers and entropy

R. L. C. Vink\* and G. T. Barkema

*Institute for Theoretical Physics, Utrecht University,  
Leuvenlaan 4, 3584 CE Utrecht, the Netherlands*

(Dated: December 10, 2002)

A Monte Carlo method is presented for the simulation of vitreous silica. Well-relaxed networks of vitreous silica are generated containing up to 300,000 atoms. The resulting networks, quenched under the BKS potential, display smaller bond-angle variations and lower defect concentrations, as compared to networks generated with molecular dynamics. The total correlation functions  $T(r)$  of our networks are in excellent agreement with neutron scattering data, provided that thermal effects and the maximum inverse wavelength used in the experiment are included in the comparison. A procedure commonly used in experiments to obtain coordination numbers from scattering data is to fit peaks in  $rT(r)$  with a gaussian. We show that this procedure can easily produce incorrect results. Finally, we estimate the configurational entropy of vitreous silica.

PACS numbers: 61.43.Fs, 61.43.Bn, 61.12.Bt

## I. INTRODUCTION

If liquid silica ( $\text{SiO}_2$ ) is cooled below its melting temperature, it usually does not crystallize, but stays a supercooled liquid for an extended period of time. Upon further cooling, to below a certain temperature known as the glass transition temperature  $T_g$ , it becomes highly viscous and shows many properties of ordinary solids, but stays disordered and does not evolve to the thermodynamically stable crystalline phase, at least on earthly time scales. The study of silica in its disordered phase (vitreous silica) is hampered by a lack of knowledge on its microscopic structure. Experimental techniques alone, such as neutron and X-ray scattering, which can uniquely resolve the structure of a crystal, are less successful in this case because of the lack of a repeating unit cell. Typically, only information averaged over many atoms, such as the radial distribution function, can be obtained from experiments.

An alternative method to study vitreous silica is through computer simulations. The usual computational approach to generate vitreous silica structures is to simulate a quench from the melt within the framework of molecular dynamics (MD). This resembles closely the experimental process used to prepare vitreous silica, except that the typical computational cooling rates are about ten orders of magnitude faster than experimental ones. In agreement with experiment, these MD simulations result in structures of vitreous silica in which almost all silicon atoms are bonded to four oxygen atoms and almost all oxygen atoms are bonded to two silicon atoms, without any sign of long-range order [1]. This in turn is in agreement with the continuous random network (CRN) model, proposed by Zachariasen [2].

The high cooling rates used in MD simulations result in structures with a strain higher than observed in experiments. This shows up, for instance, as an anomalously high density of coordination defects and a larger spread in bond lengths and bond angles. In this paper we present an alternative approach to generate models of vitreous silica. In contrast to MD, we do not attempt to simulate the details of the dynamics of the melt-quenching process. Instead, we use a Monte Carlo (MC) scheme with an artificial dynamics consisting of *bond transpositions*. Our scheme is similar in spirit to the one used by Tu *et al.* in their study of silica and silica sub-oxides [3, 4], which in turn is based on the algorithm of Wooten, Winer and Weaire (WWW) for the generation of four-fold coordinated CRNs [5, 6].

The outline of this paper is as follows. We first describe the MC scheme used by Tu *et al.* We then move on to describe a number of optimizations to this algorithm. These optimizations allow us to generate large and well-relaxed silica networks containing up to 300,000 atoms. The properties of these networks are discussed and compared to MD-prepared networks and experiment in Section VI. We end with a number of conclusions in Section VIII.

## II. BOND-SWITCHING ALGORITHM FOR SILICA

In the approach followed by Tu and co-workers, a vitreous silica network consists of  $N_s$  silicon atoms and  $N_o = 2N_s$  oxygen atoms. The total number of atoms in the network thus equals  $N = N_s + N_o$ . At all times, an explicit list of bonds is maintained which uniquely determines the connectivity or topology of the network. In the list of bonds, each silicon atom is bonded to four oxygen atoms, and each oxygen atom is bonded to two silicon atoms. The total number of bonds in the list thus equals  $4N_s$ .

---

\*Electronic address: vink@phys.uu.nl; URL: <http://www.phys.uu.nl/~vink>

To calculate energy and forces the following potential is used:

$$E_{TT} = \frac{1}{2} \sum_i k_b (b_i - b_0)^2 + \frac{1}{2} \sum_{i,j} k_\theta (\cos \theta_{ij} - \cos \theta_0)^2, \quad (1)$$

where the first summation runs over the list of bonds, and the second summation over all pairs of bonds that share one atom;  $b_i$  represents the length of the  $i$ -th bond, and  $\theta_{ij}$  is the angle between bonds  $i$  and  $j$  (which share one atom). The potential parameters for the two-body Si-O interaction are given by  $k_b = 27.0$  eV and  $b_0 = 1.60$  Å. For the three-body O-Si-O interaction common values are  $k_\theta = 4.32$  eV and  $\cos \theta_0 = -1/3$ ; for Si-O-Si interactions these values are  $k_\theta = 0.75$  eV and  $\cos \theta_0 = -1$ . Since the number of bonds in the network grows linearly with the number of atoms it contains, each energy evaluation is an  $O(N)$  operation.

The network is evolved by making explicit changes in the list of bonds, each time followed by a local energy minimization with respect to the geometric coordinates of all atoms (using for example the method of steepest descent). The changes in the list of bonds consist of bond transpositions as illustrated in Fig. 1. Each bond transposition is accepted with the Metropolis acceptance probability [7]:

$$P_a = \min \left[ 1, \exp \left( \frac{E_b - E_f}{k_B T} \right) \right], \quad (2)$$

where  $k_B$  is the Boltzmann constant,  $T$  is the temperature, and  $E_b$  and  $E_f$  are the (minimized) energies of the network before and after the proposed bond transposition.

### III. OPTIMIZED BOND-SWITCHING ALGORITHM FOR SILICA

We have optimized the bond-switching algorithm of Tu *et al.* for the generation of large and well relaxed silica networks. These optimizations are similar in spirit to the optimizations used in the scalable WWW algorithm [8, 9].

The first optimization is aimed at reducing the CPU time spent on rejected bond transpositions. After a bond transposition in the original algorithm, the energy of the network is always completely minimized. After the minimization, the bond transposition is either accepted or rejected based on the Metropolis probability.

In contrast, we reformulate the Metropolis algorithm. We first determine a threshold energy  $E_t = E - k_B T \ln(1 - r)$ , where  $r$  is a random number uniformly drawn from the interval  $[0, 1)$ . We then proceed with the minimization procedure. During minimization, the converged energy is continuously estimated. Assuming that

the total energy is harmonic around the minimum with curvature  $c$ , the energy  $E(\vec{R}_0)$  at the (unknown) minimum  $\vec{R}_0$  can be estimated from a nearby configuration  $\vec{R}$  as  $E(\vec{R}_0) \approx E(\vec{R}) - |\vec{F}|^2/c$ , with  $|\vec{F}|$  the magnitude of the total force at  $\vec{R}$ . Minimization is aborted as soon as it becomes clear that the threshold energy will not be reached and the bond transposition will be rejected. This leads to a large reduction in the number of force evaluations associated with rejected bond transpositions.

The second optimization is aimed at exploiting the local nature of the bond transposition depicted in Fig. 1. Immediately after a bond transposition, only a small cluster of atoms in the network will experience a significant force. This cluster consists of the atoms directly involved in the bond transposition, marked  $\{S1, S2, O1, O2, O3\}$  in Fig. 1, and of nearby atoms (typically extending to the fourth neighbor shell around these five transposition atoms). The number of atoms in such a cluster is about 400. It therefore suffices to calculate the force *locally* (only for the 400 or so atoms inside the cluster) rather than *globally* (for all the atoms in the network). Calculating the force on a cluster of atoms is an  $O(1)$  operation, which means that it is independent of the total number of atoms in the network. Local force calculations are therefore much cheaper than global  $O(N)$  force calculations.

Already after a converged local minimization, it is often clear that the threshold energy will not be reached, and the bond transposition can be rejected. If this is not the case, a few global minimization steps are required additionally, usually resulting in an accepted bond transposition. The combination of these two improvements reduces the computational effort from  $O(N)$  operations per attempted bond transposition to  $O(1)$  operations per attempted bond transposition, plus a few  $O(N)$  operations per accepted bond transposition. Since common acceptance probabilities are well below 1%, the speed-up for large systems is about two orders of magnitude.

### IV. INITIAL CONFIGURATIONS

The optimized bond-switching algorithm for silica requires an initial network, which should be free of coordination defects and crystalline regions. As noted in Ref. 10, four-fold coordinated CRNs decorated with one oxygen atom on each bond already provide structures that compare reasonably well to vitreous silica. As initial network we therefore use a periodic, four-fold coordinated CRN generated as described in Refs. [8, 9]. This CRN serves as the silicon backbone. Next, one oxygen atom is placed on the center of each Si-Si bond to obtain a properly coordinated silica network. The simulation volume is then scaled to obtain the experimental density of silica  $\rho = 2.20$  g cm<sup>-3</sup> [11].

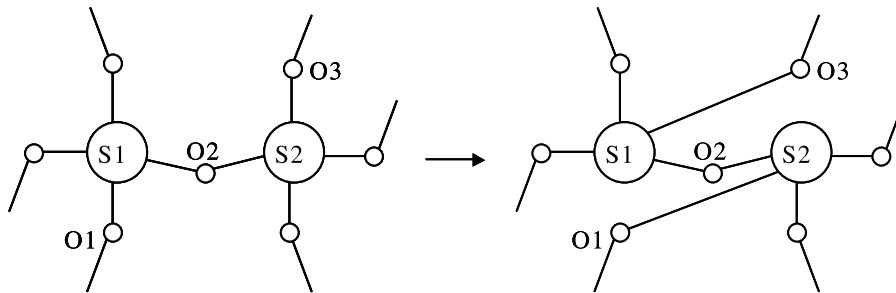


FIG. 1: Bond transposition used in the generation of vitreous silica structures. Two silicon atoms  $\{S1, S2\}$  and three oxygen atoms  $\{O1, O2, O3\}$  are selected following the geometry shown left. Next, bonds  $S1 - O1$  and  $S2 - O3$  are broken and two new bonds  $S1 - O3$  and  $S2 - O1$  are created to obtain the geometry shown right. After the bond transposition, the geometric coordinates of the atoms are relaxed (not shown).

## V. BKS SAMPLING

A computationally more expensive, but also more realistic potential for silica is the BKS potential [12]:

$$E_{BKS} = \sum_{i < j} \left( \frac{q_i q_j}{r_{ij}} + A_{ij} \exp(-B_{ij} r_{ij}) - \frac{C_{ij}}{r_{ij}^6} \right), \quad (3)$$

where the sum runs over all pairs of atoms in the system,  $r_{ij}$  is the distance between atoms  $i$  and  $j$ , and  $q_i$  is the charge of atom  $i$ . The atomic charges and the values of the potential parameters  $A_{ij}$ ,  $B_{ij}$  and  $C_{ij}$  are also listed in Ref. 12. We use the fast multipole code developed at Duke University [13] to compute the Coulomb and van der Waals interactions. The exponential term is truncated at 5.50 Å and then shifted, as described in Ref. 1.

The bond-switching algorithm described above generates networks that are local energy minima according to the potential of Tu *et al.* The algorithm can be changed such that these networks will be sampled from the Boltzmann distribution according to the BKS potential at temperature  $T$ . To this end, the acceptance probability of Eq. (2) is replaced by:

$$P = \min \left[ 1, \exp \left( -\frac{\Delta E_{TT}}{k_B T'} \right) \right] \times \min \left[ 1, \exp \left( \frac{\Delta E_{TT}}{k_B T'} - \frac{\Delta E_{BKS}}{k_B T} \right) \right], \quad (4)$$

where  $\Delta E_{TT}$  and  $\Delta E_{BKS}$  are the energy differences between the networks before and after the bond transposition, calculated with the potential of Tu *et al.* and the BKS potential, respectively. The algorithm satisfies detailed balance, also when the fictitious temperatures  $T$  and  $T'$  are different. In the expression above, the first factor biases moves according to the potential of Tu *et al.* at temperature  $T'$ , after which the second factor corrects for the difference between this potential at temperature  $T'$  and the BKS potential at temperature  $T$ .

With the above probability, bond transpositions that are accepted with the potential of Tu *et al.* undergo an

additional accept/reject decision based on the BKS potential. By increasing the temperature  $T'$  we can increase the number of moves that will be accepted under the potential of Tu *et al.* In the limit  $T' \rightarrow \infty$ , all such moves are accepted. In this limit, the accept/reject decision is based solely on the BKS potential and  $T$ . While correct, this situation is undesirable because BKS energy evaluations are expensive. In practice, a lower  $T'$  is used and the temperatures  $\{T, T'\}$  are tuned to maximize the decrease of the BKS energy of the network as a function of simulation time.

## VI. RESULTS

We have used the optimized bond-switching algorithm described in Section III to generate vitreous silica networks containing 3000 atoms ('3k'), 60,000 atoms ('60k') and 300,000 atoms ('300k'). For the 3000-atom and the 60,000-atom networks the bond-switching algorithm was used in conjunction with BKS sampling at temperatures  $k_B T = 0.30$  eV and  $k_B T' = 0.70$  eV (see Section V). For the 300,000-atom network, BKS sampling proved to be too computationally demanding and was not implemented; for this network the Metropolis probability of Eq. (2) was used with  $k_B T = 0.15$  eV and the potential of Tu *et al.*

All three networks were evolved with approximately 10 attempted bond transpositions per atom from their starting configurations. The energy of the resulting networks was then minimized in a single quench using the method of steepest descent and the BKS potential without volume optimization. We observed that if volume optimization were used with the BKS potential, the density of the networks becomes unphysically high, typically in the range 2.27-2.37 g cm<sup>-3</sup>. Similar high densities are also reported in a number of MD studies [1, 14].

In Fig. 2 we show the radial distribution functions (RDFs)  $g_{SiSi}(r)$ ,  $g_{SiO}(r)$ , and  $g_{OO}(r)$  for model '60k'. The RDFs are density normalized such that  $\lim_{r \rightarrow \infty} g_{\alpha\beta}(r) = 1$ . The RDFs for models '3k' and

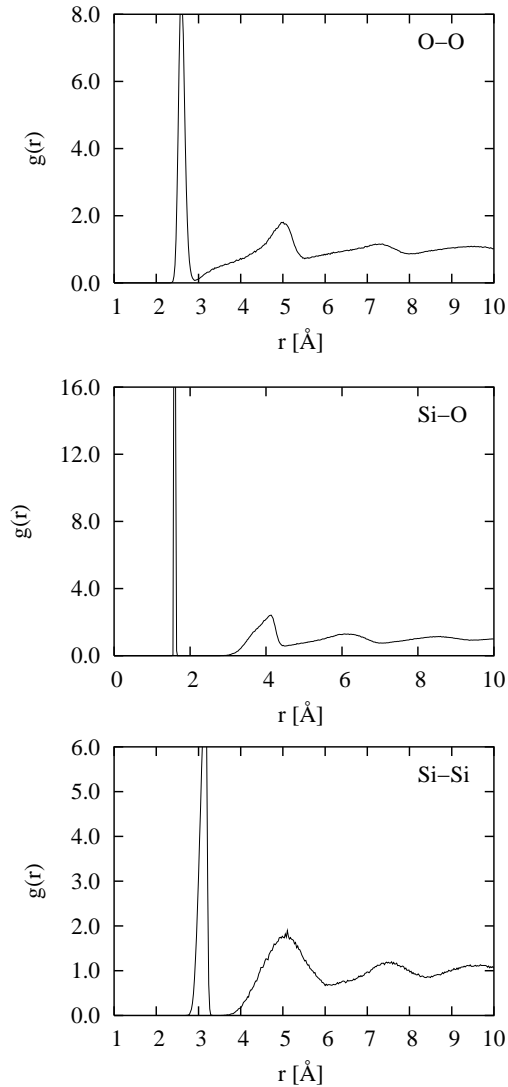


FIG. 2: Species-dependent density-normalized radial distribution functions  $g_{\alpha\beta}(r)$  for network ‘60k’ after relaxation at zero temperature with the BKS potential [12].

‘300k’ are similar (not shown).

The Si-O RDF was used to extract a cutoff for the Si-O bond length at  $r_c = 1.80 \text{ \AA}$ , where  $r_c$  is taken at the minimum between the first and the second peak. Based on this  $r_c$  we find structural properties as reported in Table I. For comparison, we also report results obtained with MD using the same BKS potential. Compared to MD, we observe that our networks are better relaxed, as is evident from the smaller variations in the O-Si-O and Si-O-Si bond angles. Moreover, our networks are nearly free of coordination defects.

A more stringent test is to compare the properties of our networks to experimental data. The crucial quantity to consider is the total correlation function  $T(r)$  as

TABLE I: Structural and energetic properties of our vitreous silica networks at zero temperature, after a local energy minimization under the BKS potential at the experimental density. For comparison we also report properties of silica networks prepared by a quench to zero temperature under MD [1] using the same potential. The number of atoms in each structure is given by  $N$ ;  $E$  is the BKS energy per silicon atom in eV;  $\rho$  is the density in  $\text{g cm}^{-3}$ ; the Si-O bond length and its rms variation are given in  $\text{\AA}$ ; the mean bond angles and their variations (rms and FWHM) are given in degrees;  $z_4$  and  $z_2$  are the percentages of perfectly coordinated silicon and oxygen atoms, respectively, based on a Si-O bond-length cut-off at  $1.80 \text{ \AA}$ .

	‘3k’	‘60k’	‘300k’	MD
$N$	3000	60,000	300,000	1002
$E$	-58.12	-58.10	-58.09	–
$\rho$	2.20 <sup>a</sup>	2.20 <sup>a</sup>	2.20 <sup>a</sup>	2.27-2.37
Si-O				
mean	1.606	1.608	1.606	1.595 <sup>b</sup>
rms	0.010	0.011	0.011	–
O-Si-O				
mean	109.44	109.43	109.43	108.3
rms	3.95	4.59	4.32	–
FWHM	8.3	9.3	9.8	12.8
Si-O-Si				
mean	153.89	153.57	153.00	152
rms	11.75	11.72	11.94	–
FWHM	34	33.3	34.5	35.7
$z_4$	100%	100%	99.997%	99.8%
$z_2$	100%	100%	99.998%	99.8%

<sup>a</sup>Fixed to the experimental density  $\rho = 2.20 \text{ g cm}^{-3}$  [11].

<sup>b</sup>Location of the first peak in the Si-O RDF.

obtained in X-ray or neutron scattering experiments. In these experiments, the quantity that can be measured directly is the total interference function  $Q_i(Q)$ ; the correlation function  $T(r)$  is obtained via a Fourier transform of  $Q_i(Q)$ . In practice, the resolution in  $T(r)$  is determined by the maximum attainable inverse wavelength  $Q_{max}$  in the experiment. As discussed in Ref. 15, peaks in  $T(r)$  are significantly broadened because  $Q_{max}$  is not infinite in real experiments. In addition to Fourier broadening, there is thermal broadening because experiments are typically carried out at room temperature. For a meaningful comparison it is essential to take these factors into account.

To capture the effect of thermal broadening, all three networks are thermalized over approximately 1 ps with MD using the BKS potential in the NVE-ensemble at  $T \approx 300 \text{ K}$ . The structural properties of the thermalized networks are summarized and compared to experiment in Table II. We observe good agreement on the Si-O bond length, the variation in the bond length and the mean bond angles. Compared to experiment, our networks slightly overestimate the variation in the O-Si-O bond angle. This may indicate that experimental vitreous silica is more relaxed than our networks. Experimen-

TABLE II: Structural properties of networks ‘3k’, ‘60k’ and ‘300k’ after thermalization at 300 K, based on a Si-O bond-length cut-off at 1.80 Å. Shown are the mean Si-O bond length with rms variation in Å; the mean bond angles with rms variation and FWHM of the corresponding distribution in degrees; and the mean coordination number  $z$  of silicon atoms. For comparison we also report values obtained in experiments.

	‘3k’	‘60k’	‘300k’	Experiment
Si-O				
mean	1.610	1.614	1.612	1.609 [19]
rms	0.042	0.042	0.041	0.047 [19]
O-Si-O				
mean	109.38	109.37	109.37	109.7 ± 0.6 [19]
rms	5.79	6.27	6.31	4.5 [19]
FWHM	13.1	14.4	14.5	–
Si-O-Si				
mean	153.01	152.74	152.20	148 [16]; 152 [22]
rms	12.22	12.31	12.60	7.5 [23]
FWHM	35	34.4	36.2	12.8 [16]; 26 [24]; 36 [17]
$z$	4.000	4.000	4.000	–

tal estimates for the variation in the Si-O-Si bond angle range from 12.8 degrees [16] to 36 degrees [17]. Compared to these data our networks coincide with the higher value. The coordination numbers reported in Table II indicate that the vast majority of atoms is still properly coordinated after thermalization.

Next, Fourier broadening is taken into account. In the absence of Fourier broadening, the total correlation function of a network is simply a weighted sum of the RDFs:

$$T(r) = \frac{r}{w_{SiSi} + w_{SiO} + w_{OO}} [w_{SiSi} \times g_{SiSi}(r) + w_{SiO} \times g_{SiO}(r) + w_{OO} \times g_{OO}(r)], \quad (5)$$

in which each RDF is normalized such that  $\lim_{r \rightarrow \infty} T(r) = r$ . We focus on neutron scattering, in which case the weights are given by:  $w_{SiSi} = 0.1722$ ,  $w_{SiO} = 2 \times 0.4817$  and  $w_{OO} = 4 \times 0.3370$ , see Ref. 15. These weights include the neutron scattering lengths of silicon and oxygen atoms; the factors of 2 and 4 account for the chemical composition of silica (two oxygen atoms for every silicon atom).

To obtain the Fourier-broadened correlation function  $T_b(r)$ , the correlation function of Eq. (5) is transformed to obtain the interference function  $Qi(Q)$ :

$$Qi(Q) = \int_{r=0}^{r=r_{max}} [T(r) - r] \sin(Qr) dr, \quad (6)$$

where  $r_{max}$  is half the edge of the cubic simulation volume of the model. Next, we transform the interference function back to obtain  $T_b(r)$ :

$$T_b(r) = r + \frac{2}{\pi} \int_{Q=0}^{Q=Q_{max}} M(Q) Qi(Q) \sin(Qr) dQ, \quad (7)$$

using the experimentally relevant  $Q_{max}$ . The function  $M(Q)$  is an (optional) modification function commonly used to reduce Fourier artifacts. A popular choice is the Lorch modification function [18] given by:

$$M(Q) = \frac{Q_{max}}{\pi Q} \sin\left(\frac{\pi Q}{Q_{max}}\right). \quad (8)$$

The neutron  $T(r)$  of vitreous silica was accurately measured by Grimley, Wright and co-workers in 1991 [19, 20] using high-energy neutrons with  $Q_{max} = 45.2 \text{ \AA}^{-1}$ . For each of the three thermalized networks we determined the Fourier-broadened correlation function  $T_b(r)$  using the same value for  $Q_{max}$  and the Lorch modification function. The experimental correlation function and the correlation function of the thermalized ‘60k’ network are compared to each other in Fig. 3. We observe excellent agreement. As a more quantitative measure of the agreement between model and experiment we consider the  $R_\chi$  factor [15] defined as:

$$R_\chi^2 = \frac{\int [T_{exp}(r) - T_{model}(r)]^2 dr}{\int T_{exp}^2(r) dr}. \quad (9)$$

The discrepancy between the experimental  $T(r)$  and  $T_b(r)$  of the thermalized ‘60k’ network, over the range  $1.0 \leq r \leq 10.0 \text{ \AA}$ , equals  $R_\chi = 5.1\%$ . For the thermalized networks ‘3k’ and ‘300k’ we obtain  $R_\chi$  factors of 4.7% and 4.9%, respectively, over the same range.

In the top frame of Fig. 4 we compare the total interference function of the thermalized ‘60k’ network to experiment. There is excellent agreement on the overall peak positions and also on the damping of the interference function for large  $Q$ . We observe some discrepancy at  $Q \approx 15 \text{ \AA}^{-1}$ , where the small peak visible in the experimental data is not reproduced by our network. The discrepancy seems to be temperature-related: the lower frame of Fig. 4 shows that the network at zero temperature does reproduce the peak correctly.

We observe in Fig. 3 that the total correlation function is significantly broadened by Fourier and thermal effects, in particular the first peak at  $r \approx 1.6 \text{ \AA}$ . We have quantified the broadening of this peak by fitting it to the form:

$$P(r) = \frac{1}{\sqrt{2\pi}} \frac{\eta}{r\sigma} \exp\left[-\frac{(r-r_0)^2}{2\sigma^2}\right], \quad (10)$$

with fit parameters  $\{r_0, \sigma, \eta\}$ . This follows the same procedure used in Ref. 19 to obtain bond lengths and coordination numbers from experimentally obtained correlation functions. The parameters  $r_0$  and  $\sigma$  provide estimates for the mean Si-O bond length and its variation. The parameter  $\eta$  can be used to extract the mean coordination number  $z$  of silicon atoms:

$$z = 4\pi\eta\rho_O \frac{w_{SiSi} + w_{SiO} + w_{OO}}{w_{SiO}}, \quad (11)$$

with  $\rho_O$  the number density of oxygen atoms,  $w_{\alpha\beta}$  the neutron weights and  $T(r)$  normalized such that  $\lim_{r \rightarrow \infty} T(r) = r$ .

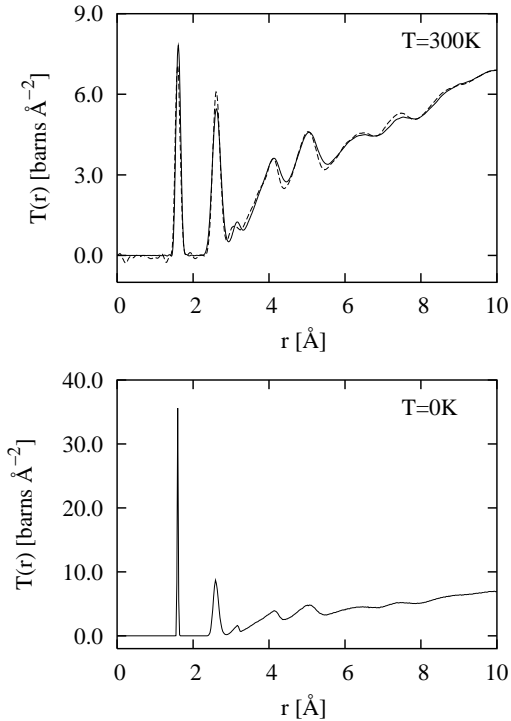


FIG. 3: Total neutron correlation function  $T(r)$  of vitreous silica. The top frame shows the Fourier-broadened correlation function of thermalized network ‘60k’ (solid) compared to the experimental result of Wright and co-workers (dashed) taken from Ref. 20. The lower frame shows the correlation function of the same network at zero temperature without Fourier broadening.

The effects of Fourier and thermal broadening on the parameters  $\{r_0, \sigma, z\}$  are reported in Table III. As expected, the broadening is significant: the combined effect of Fourier and thermal broadening will boost  $\sigma$  by a factor of over five.

It is also interesting to compare the silicon coordination number obtained directly from the atomic coordinates of a network, to that obtained from a fit to the correlation function of that network. To this end the data of the networks at 300 K without Fourier broadening in Table III are compared to Table II. The fitting procedure accurately predicts the Si-O bond length and its variation  $\sigma$ , but not the coordination number which we know to be 4.000. This result is important because it shows that in the ideal situation free of Fourier broadening, fits based on Eq. (10) will systematically underestimate the coordination number. The cause of this underestimation is due to the non-gaussian nature of the peak in  $rT(r)$ : fitting with a more elaborate function, for instance with a sum of two gaussians, yields the correct coordination number. The table also shows that fits with Eq. (10) applied to Fourier-broadened data tend to overestimate the coordination numbers.

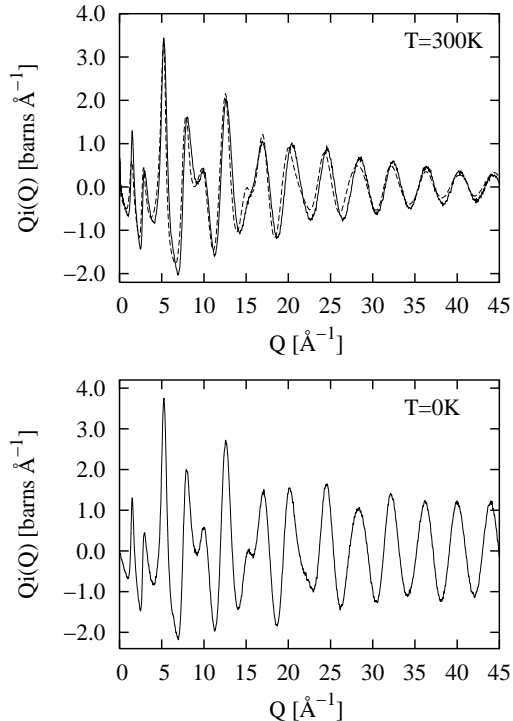


FIG. 4: Total neutron interference function  $Q_i(Q)$  of vitreous silica. The top frame shows  $Q_i(Q)$  of thermalized network ‘60k’ (solid) compared to experimental data (dashed) of Grimley and co-workers [19]. The lower frame shows the interference function of network ‘60k’ at zero temperature.

TABLE III: The effect of Fourier broadening (FB) and thermal broadening on the optimal parameters  $\{r_0, \sigma, z\}$  obtained from a fit of Eq. (10) to the first peak in  $T(r)$  of our networks. Network ‘3k’ proved to be too small to accurately sample the first peak and was not used in this comparison. The parameters  $r_0$  and  $\sigma$  are given in  $\text{\AA}$ .

		‘60k’	‘300k’
$T = 0$ K no FB	$r_0$	1.607	1.601
	$\sigma$	0.011	0.011
	$z$	$3.962 \pm 0.011$	$3.980 \pm 0.004$
$T = 0$ K with FB	$r_0$	1.609	1.607
	$\sigma$	0.048	0.048
	$z$	$4.155 \pm 0.052$	$4.161 \pm 0.053$
$T = 300$ K no FB	$r_0$	1.611	1.610
	$\sigma$	0.041	0.040
	$z$	$3.977 \pm 0.013$	$3.978 \pm 0.011$
$T = 300$ K with FB	$r_0$	1.614	1.612
	$\sigma$	0.060	0.060
	$z$	$4.046 \pm 0.019$	$4.048 \pm 0.019$

## VII. CONFIGURATIONAL ENTROPY

Recently, we developed a method to determine the configurational entropy of a network [21]. The method requires only the atomic coordinates and a list of bonds between particles, for a single well-relaxed configuration. In the original paper, the method was applied to a silica network consisting of 3000 atoms. Starting with the atomic coordinates of this network, the list of bonds was constructed using  $r_c = 1.80 \text{ \AA}$  for the Si-O bond-length cutoff. Each Si-O-Si bridge was replaced by a single Si-Si bond. We then applied our method to the resulting silicon backbone network to obtain for the configurational entropy  $s = 0.88 k_B$  per silicon atom.

The accuracy of the method is sensitive to the size of the network. As mentioned in the original paper, the configurational entropy of vitreous silica reported above is most likely an underestimate due to the limited size of that network. The large networks generated in this work allow us to quantify these finite size effects. They also allow us to determine the minimum size of a network that is required to accurately measure the configurational entropy.

To this end, we use our method to determine the entropy of networks ‘3k’, ‘60k’ and ‘300k’ in two different ways: first, by using the entire simulation volume of the network; secondly, by using only half the volume of the simulation cell. The first procedure yields entropies of 0.83, 0.99 and  $1.04 k_B$  per silicon atom, respectively, while the second procedure yields 0.78, 0.97 and  $1.03 k_B$  per silicon atom, respectively. This illustrates that finite-size effects are significant for the smallest network, but

small for the large ones. Most of the difference in entropy between the three networks is due to the varying degree of relaxation in these networks.

## VIII. CONCLUSIONS

In summary, we have presented a Monte Carlo-based approach for the generation of well-relaxed networks of vitreous silica, based on earlier work of Tu *et al.* With this method, networks containing 3000, 60,000 and 300,000 atoms are generated. Compared to networks generated with molecular dynamics, our networks have smaller bond-angle variations and are nearly defect-free, indicating they are better relaxed.

The total correlation function  $T(r)$  of our networks is in excellent agreement with neutron scattering experiments (with  $R_\chi$  factors around 5%), provided that thermal effects and the maximum experimental inverse wavelength  $Q_{max}$  are included in the comparison. We also determined the silicon coordination number of our networks by fitting a gaussian to  $rT(r)$ , as is commonly done in experiments. We observe that the results of this procedure are biased to lower numbers by the non-gaussian nature of the peaks, and to higher numbers due to finite value of  $Q_{max}$ . The configurational entropy of vitreous silica was determined to be  $0.99 k_B$  and  $1.04 k_B$  per silicon atom, for the networks containing 60,000 and 300,000 atoms, respectively.

Upon request, we will communicate the atomic coordinates of our networks.

- 
- [1] K. Vollmayr, W. Kob, and K. Binder, Phys. Rev. B **54**, 15808 (1996).
  - [2] W. H. Zachariasen, J. Am. Chem. Soc. **54**, 3841 (1932).
  - [3] Yuhai Tu, G. Grinstein, and David Vanderbilt, Phys. Rev. Lett. **81**, 4899 (1998).
  - [4] Yuhai Tu and J. Tersoff, Phys. Rev. Lett. **84**, 4393 (2000).
  - [5] F. Wooten, K. Winer, and D. Weaire, Phys. Rev. Lett. **54**, 1392 (1985).
  - [6] B. R. Djordjević, M. F. Thorpe, and F. Wooten, Phys. Rev. B **52**, 5685 (1995).
  - [7] N. Metropolis, A. W. Rosenbluth, M. N. Rosenbluth, A. H. Teller, and E. Teller, J. Chem. Phys. **21**, 1087 (1953).
  - [8] G. T. Barkema and N. Mousseau, Phys. Rev. B **62**, 4985 (2000).
  - [9] R. L. C. Vink, G.T. Barkema, M.A. Stijnman, and R.H. Bisseling, Phys. Rev. B **64**, 245214 (2001).
  - [10] M. F. Thorpe and S. W. de Leeuw, Phys. Rev. B **33**, 8490 (1986).
  - [11] O. V. Mazurin, M. V. Strelina, and T. P. Shvaikovskaya, *Handbook of Glass Data* (Elsevier, Amsterdam, 1983), Pt. A.
  - [12] B. W. H. van Beest, G. J. Kramer, and R. A. van Santen, Phys. Rev. Lett. **64**, 1955 (1990).
  - [13] W. T. Rankin and J. A. Board, Technical Report 95-002, Department of Electrical Engineering, Duke University (1995).
  - [14] J. Horbach and W. Kob, Phys. Rev. B **60**, 3169 (1999).
  - [15] A. C. Wright, J. Non-Cryst. Solids **179**, 84 (1994).
  - [16] P. Grandinetti, based on recent NMR measurements, private communication (2002).
  - [17] R. L. Mozzi and B. E. Warren, J. Appl. Crystallogr. **2**, 164 (1969).
  - [18] E. A. Lorch, J. Phys. C2, 229 (1969).
  - [19] D. I. Grimley, A. C. Wright, and R. N. Sinclair, J. Non-Cryst. Solids **119**, 49 (1990).
  - [20] A. C. Wright, R. A. Hulme, D. I. Grimley, R. N. Sinclair, S. W. Martin, D. L. Price, and F. L. Galeener, J. Non-Cryst. Solids **129**, 213 (1991).
  - [21] R. L. C. Vink and G. T. Barkema, Phys. Rev. Lett. **89**, 76405 (2002).
  - [22] P. G. Coombs, J. F. De Natale, P. J. Hood, E. K. McElfresh, R. S. Wortman, and J. F. Schackelford, Philos. Mag. **51**, L39 (1985).
  - [23] J. Neufeind and K. D. Liss, Ber. Bunsengesellschaft **100**, 1341 (1996).
  - [24] R. F. Pettifer, R. Dupree, I. Farnan, and U. Sternberg, J. Non-Cryst. Solids **106**, 408 (1988).